Journal of Power Sources 315 (2016) 199–208

Contents lists available at ScienceDirect

Journal of Power Sources

journal homepage: www.elsevier.com/locate/jpowsour

Probability based remaining capacity estimation using data-driven and neural network model

Yujie Wang, Duo Yang, Xu Zhang, Zonghai Chen*

Department of Automation, University of Science and Technology of China, Hefei 230027, PR China

HIGHLIGHTS

- The data-driven model is established for battery state-of-charge estimation.
- The neural network model is established for battery state-of-energy estimation.
- The probability based estimation method is employed for battery state estimation.
- The HPPC/DST/UDDS profiles are performed for experiment verification.

ARTICLE INFO

Article history:
Received 12 January 2016
Received in revised form
6 March 2016
Accepted 15 March 2016
Available online 22 March 2016

Keywords:
Electric vehicle
Battery state estimation
Data-driven approach
Neural network model

ABSTRACT

Since large numbers of lithium-ion batteries are composed in pack and the batteries are complex electrochemical devices, their monitoring and safety concerns are key issues for the applications of battery technology. An accurate estimation of battery remaining capacity is crucial for optimization of the vehicle control, preventing battery from over-charging and over-discharging and ensuring the safety during its service life. The remaining capacity estimation of a battery includes the estimation of state-of-charge (SOC) and state-of-energy (SOE). In this work, a probability based adaptive estimator is presented to obtain accurate and reliable estimation results for both SOC and SOE. For the SOC estimation, an *n* ordered RC equivalent circuit model is employed by combining an electrochemical model to obtain more accurate voltage prediction results. For the SOE estimation, a sliding window neural network model is proposed to investigate the relationship between the terminal voltage and the model inputs. To verify the accuracy and robustness of the proposed model and estimation algorithm, experiments under different dynamic operation current profiles are performed on the commercial 1665130-type lithium-ion batteries. The results illustrate that accurate and robust estimation can be obtained by the proposed method.

1. Introduction

Energy and environmental crisis have long been challenges facing the world's automobile industry. The grim energy and environmental situation around the world has accelerated the strategic transformation of transportation and energy technology. Therefore, new energy vehicles such as the battery electric vehicles (BEV), hybrid electric vehicles (HEV), and fuel cell electric vehicles (FCEV) are generally considered as good candidates to replace conventional internal combustion engine vehicles. With the advantages of high energy density, environmentally benign features, wide operating temperature range, low self-discharge rate and long cycle life, the lithium-ion batteries have become widely used in electric vehicles in recent years. Since large numbers of lithium-ion batteries are composed in pack and the batteries are complex electrochemical devices with a distinct nonlinear behavior depending on various internal and external conditions, their monitoring and safety concerns are key issues for the application of battery technology [1].

As a key component to the battery power system, the battery management systems (BMS) are designed to provide monitoring, diagnosis, control and protecting functions to enhance the operation of the battery packs [2]. An intelligent BMS is always developed based on practicality with the characteristics of universality, intelligent, individuation, friendly interaction and has to be extensible in almost certain cases that more features can be added if

* Corresponding author.
E-mail address: chenzh@ustc.edu.cn (Z. Chen).

http://dx.doi.org/10.1016/j.jpowsour.2016.03.054
0378-7753/

necessary. Fig. 1 gives a block diagram of key technologies in BMS. As can be seen from the figure, the key technologies of the BMS can be summarized into three parts: (1) Battery state estimation. In an intelligent BMS, the battery performance is not only evaluated by the state-of-charge (SOC), but also evaluated from the state-of-energy (SOE) and other indicators to realize a comprehensive and accurate estimation. (2). Battery equalization. When a battery pack is first constructed, the capacities of each component cell can be well matched. However as time goes by, individual cells lose capacity at different degrees due to temperature variations and other factors. The weak cells effectively limit the run time of the battery pack. When the pack is charged, the weak cells reach the overcharge voltage limit before others, so other cells are not charged to their maximum available capacity. Likewise, when the pack is discharged, the weak cells reach their cut-off voltage sooner than the others and shorten the overall working time of the battery pack. Therefore the battery equalization circuits and algorithms are required to extend battery life, improve the cell consistency and efficiency. (3) Battery safe and efficient management. The battery management systems on modern electric vehicles are always distributed structured on high-speed Controller Area Network (CAN) bus. The battery parameters detection is expanded from voltage, current and temperature to connection, insulation, smoke, collision and so on. The fault diagnosis of BMS involves sensor fault, actuator fault, network fault, over charge, over discharge, over current, temperature anomaly, insulation fault, uniformity fault and so on. Battery safe and efficient management also involves safe charge/discharge control, battery thermal management, key data storage and analysis.

The SOC which reflects the residual capacity of the battery is not directly measurable and should be estimated by other approaches. Many methods have been proposed in the literature for battery states estimation [3–37]. The coulomb counting (ampere-hour integral) method is one of the most simple and general way [3]. Low-cost sensors for current measurement are available to achieve this method, and the required computing of this method is very low so that it can be generalized in different types of application scenarios. This approach is also possible and easy to be combined with other techniques such as the model based estimation approaches. However, it has accumulated error since there are inevitable sensor noise and measurement drift. This approach is also hard to calibrate the initial error and cannot get the precise initial SOC automatically. The open-circuit voltage (OCV) based method is another approach to obtain the battery SOC [4–5]. Through this method, batteries are required to have long time resting in order to reach balance. Therefore this method is appropriate only when the EVs are parking rather than driving. The artificial neural network (ANN) method has been employed for SOC estimation in Refs. [6–11]. A remarkable disadvantage of this method is a great number of data are needed to train the network and a lot of computations are required. Meanwhile, the prediction error can be greatly influenced by the training data and the training methods. To improve the performance of SOC estimation, model based estimation approaches such as the nonlinear observer [12–15], extended Kalman filter (EKF) [16–21], sigma-point Kalman filter (SPKF) [22–23], adaptive extended Kalman filter (AEKF) [24–26], unscented Kalman filter (UKF) [27–30], particle filter (PF) [31–32], unscented particle filter (UPF) [33], invariant imbedding method [34], sliding mode observer [35–37] were proposed. With low-complexity the nonlinear observer can be used when the system is observable. The Kalman filter series of algorithms can find the optimal solution provided by nonlinear observer. However these methods require accurate model parameters, and the system noise and observation noise must satisfy the Gaussian distribution; otherwise the filter performance will decrease or even diverge. In Ref. [34], Dong et al. proposed an online estimator for SOC and parameters estimation based on the invariant imbedding method. The accuracy and robustness of the proposed method have been validated under dynamic working conditions. The sliding mode observer can suppress the disturbance and modeling error, but the chatter cannot be ignored.

The voltage levels and working plateaus of different types of batteries are entirely different. Even with the same capacity the stored energy of the batteries are bound to be very different, which will cause a corresponding difference in the useful life or mileage of vehicles. Therefore the SOE is defined to indicate the remaining

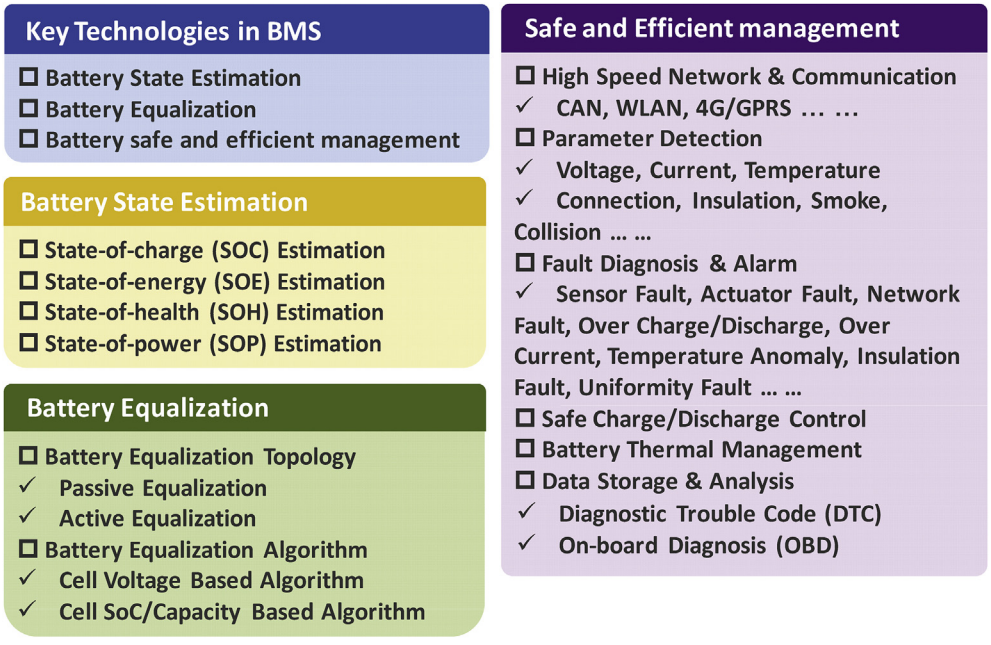

Fig. 1. Block diagram of key technologies in BMS.

available energy of the batteries. The term of "state-of-energy" [38] has been reported in literature especially in recent years [39–41]. As another key parameter of the battery system, the SOE is used to evaluate the remaining driving range and energy demand. Liu et al. [39] used the Back Propagation (BP) network to estimate the SOE at dynamic currents and temperatures and compared the difference between the SOE and SOC. He et al. [40] proposed a Gaussian model for SOE estimation. The central difference Kalman filter (CDKF) is employed to provide accurate SOE estimation result. Dong et al. [41] reported a wavelet neural network (WNN), and the BP algorithm is used for data training. However the proposed WNN model only considered the states and parameters of the last unit time.

A common feature of the model based state estimation algorithm is that these methods are highly dependent on the prediction precision of battery model. In this paper, the data-driven model and the sliding window neural network model are established for battery SOC and SOE estimation. The contributions of this work can be summarized as follows: (1) a data driven model is developed estimation by combining an n ordered RC equivalent circuit model with an electrochemical model to obtain more accurate voltage prediction results for SOC estimation. (2) A sliding window neural network model is proposed to investigate the relationship between the terminal voltage and the model inputs for the SOE estimation. (3) The Hybrid Pulse Power Characteristic (HPPC) test is performed to evaluate the model precision of the proposed data driven and neural network models. (4) The probability based estimation algorithm using Bayesian learning technology is employed for battery state estimation. To verify the accuracy and robustness of the proposed model and estimation algorithm, the Dynamic Stress Test (DST) and Urban Dynamometer Driving Schedule (UDDS) current profiles are performed on the commercial 1665130-type lithium-ion battery develop by Fujian Brother Electric CO., LTD of China. The experimental results show that accurate and robust estimation of SOC and SOE can be obtained by the proposed algorithm. This paper is organized as follows: In Section 2, the definitions of SOC and SOE are first introduced. Then we give the battery model description and the state-space equation. In Section 3, the probability based adaptive estimator is introduced and compared with the traditional Kalman filter. In Section 4, Experiments under different dynamic operation current profiles such as the DST and UDDS are performed to verify the proposed method. Finally, the conclusions are given in Section 5.

2. Model description

2.1. Definition of SOC and SOE

The SOC reflects the residual capacity of a battery, and is defined as the ratio of the remaining capacity to the maximum available capacity which can be expressed as follows [42]:

$$SoC(t) = SoC(t_0) + \eta_c \int_{t_0}^{t} i(\tau)\mathrm{d}\tau / C_n \tag{1}$$

where $SOC(t)$ is the SOC value at time t, $SOC(t_0)$ is the SOC value at initial time t_0, $i(\tau)$ represents the current at time τ, η_c represents the coulombic efficiency, C_n represents the total available capacity of the battery.

The SOE is defined to indicate the remaining available energy of the batteries, which can be expressed as the following equation [38]:

$$SoE(t) = SoE(t_0) + \eta_e \int_{t_0}^{t} P(\tau)\mathrm{d}\tau / E_n \tag{2}$$

where $SOE(t)$ is the SOE value at time t, $SOE(t_0)$ is the SOE value at initial time t_0, $P(\tau)$ represents the power at time τ, η_e denotes the energy efficiency of battery and E_n represents the total available energy of the battery. Compared with the SOC which varies linearly with the charge/discharge current, the SOE is nonlinear with the current because of the consideration of energy loss on the internal resistance, the electrochemical reactions and other factors.

2.2. Battery model

The battery models used for battery states estimation can be generally classified into three types: the electrochemical model, the equivalent circuit model and the neural network model.

2.2.1. Data-driven model

In this work, we proposed a data-driven model which is consisted by an equivalent circuit network and a combined electrochemical model. Based on the dynamic characteristics and working principles of the battery, the equivalent circuit model is developed by using resistors, capacitors, and voltage sources to form a circuit network [43]. Fig. 2 shows the schematic diagram of an equivalent circuit model with n RC networks. As can be seen from the figure, the U_{ocv} is used to denote the battery voltage source. R_{chg} and R_{dchg} represent the internal ohmic resistance when charging and discharging. R_i and C_i ($i = 1, 2, \ldots, n$) are used to denote the dynamic characteristics include polarization, diffusion, hysteresis and so on. The electrical behavior of the n RC model can be expressed as follows:

$$\begin{cases} \dot{U}_i = -U_i/R_iC_i + i/C_i \\ U_t = U_{ocv} - iR_{dchg} - \sum_{i=1}^{n} U_i \end{cases} \tag{3}$$

where i is the load current, U_t is the terminal voltage and U_i ($i = 1, 2, \ldots, n$) represents the voltage of the RC networks.

The electrochemical model based on the electrochemical mechanism of the battery can accurately reflect the characteristics of the battery OCV which includes the Shepherd model, the Unnewehr universal model, the Nernst model and the combined model. The combined model can be viewed as a combination of the previous three models to obtain the most accurate performance and can be expressed as follows:

$$\begin{aligned} U_{ocv}(t) = {} & U_{ocv,0} + K_0 SoC(t) + K_1/SoC(t) + K_2 \ln(SoC(t)) \\ & + K_3 \ln(1 - SoC(t)) \end{aligned} \tag{4}$$

where $U_{ocv,0}$ is the open-circuit voltage of a battery cell when fully charged, $U_{ocv}(t)$ is the cell terminal voltage, K_i(i = 0,1,2,3) are the

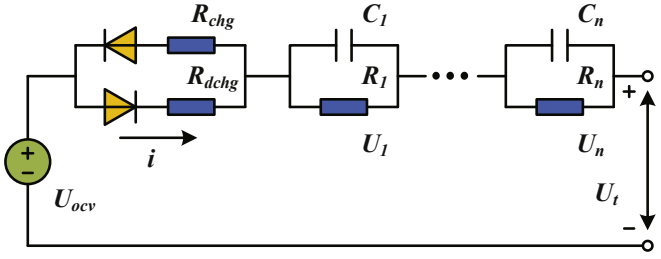

Fig. 2. Schematic diagram of the n RC equivalent circuit model.

model parameters which can be identified by the recursive least square method.

2.2.2. Neural network model

Multiple layers of neurons with nonlinear transfer functions allow the neural network to learn nonlinear and linear relationships between the input and output vectors. A single-layer network of $\boldsymbol{S}$ neurons having $\boldsymbol{R}$ inputs is shown below in Fig. 3 (a). As can be seen from the figure, each input is weighted with an appropriate $\boldsymbol{w}$. The sum of the weighted inputs and the bias forms the input to the transfer function $\boldsymbol{f}$. The neurons may use any differentiable transfer function to generate their output such as the log-sigmoid transfer function which generates outputs between 0 and 1 as the neuron's net input goes from negative to positive infinity, the tan-sigmoid transfer function which generates outputs between −1 and 1, and the linear transfer function in which the network outputs can take on any value. It should be noted that the three transfer functions described above are the most commonly used transfer functions for back-propagation, but other differentiable transfer functions can be created and used with back-propagation if necessary.

A network layer diagram with a sliding window m is used as a general function approximator of battery terminal voltage for SOE estimation as shown in Fig. 3 (b). According to the figure, the input vector of the input layer is $\boldsymbol{R}_k = [SOE_k, T_k, i_k, V_{k-1}, \ldots, i_{k-\mathrm{m}}, V_{k-1-\mathrm{m}}]^T$, and the output vector of the output layer is $\boldsymbol{Y}_k = [V_k]$. $\boldsymbol{S}$ is the number of neurons in the hidden layer. The activation functions of neurons in the hidden layer are log-sigmoid transfer functions and the function in the output layer is the linear transfer function. Thus the output of this network is shown in Eq. (5):

$$V(k) = \mathrm{purelin}\left(\mathbf{Lw}^2 \mathrm{logsig}\left(\mathbf{Iw}^1\mathbf{p} + \mathbf{b}^1\right) + \mathbf{b}^2\right) \tag{5}$$

where $\mathbf{p} = [\,SOE_k, T_k, i_k, V_{k-1}, \ldots, i_{k-\mathrm{m}}, V_{k-1-\mathrm{m}}]^T$, The weight vectors $\{\mathbf{Lw}^2, \mathbf{Iw}^1, \mathbf{b}^1, \mathbf{b}^2\}$ are parameters of this network, and they can be defined during the training phase of the network using back-propagation algorithms.

2.3. State-space equation for SOC and SOE estimation

To perform the model based SOC and SOE estimation, a state space to describe the battery model is required. In this paper we use the n RC equivalent circuit model and the combined model for SOC estimation and the sliding window neural network model for the SOE estimation. The discretization form of battery state-space equation for SOC estimation can be written as Eq. (6):

$$\begin{cases} \begin{bmatrix} U_{1,k} \\ \vdots \\ U_{n,k} \\ SoC_k \end{bmatrix} = \begin{bmatrix} \exp(-\Delta t/\tau_1) & \cdots & 0 & 0 \\ \vdots & \ddots & 0 & 0 \\ 0 & \cdots & \exp(-\Delta t/\tau_n) & 0 \\ 0 & \cdots & 0 & 1 \end{bmatrix} \begin{bmatrix} U_{1,k-1} \\ \vdots \\ U_{n,k-1} \\ SoC_{k-1} \end{bmatrix} + \begin{bmatrix} (1-\exp(-\Delta t/\tau_1))R_1 \\ \vdots \\ (1-\exp(-\Delta t/\tau_n))R_n \\ \eta_c \Delta t/C_n \end{bmatrix} i_k + \begin{bmatrix} w_{1,k}^1 \\ \vdots \\ w_{1,k}^n \\ w_{1,k}^{n+1} \end{bmatrix} \\ U_{t,k} = U_{ocv} - i_k R_{dchg} - \sum_{i=1}^{n} U_{i,k} + v_{1,k} \end{cases} \tag{6}$$

The discretization form of battery state-space equation for SOE estimation can be expressed as Eq. (7):

$$\begin{cases} SoE_k = SoE_{k-1} + \eta_e \Delta t i_k U_{t,k}/E_n + w_{2,k} \\ U_{t,k} = V_k = \mathrm{purelin}\left(\mathbf{Lw}^2 \mathrm{logsig}\left(\mathbf{Iw}^1\mathbf{p} + \mathbf{b}^1\right) + \mathbf{b}^2\right) + v_{2,k} \end{cases} \tag{7}$$

where $\{w_k\}$ and $\{v_k\}$ are the process and the measurement noises with covariance Q and R, respectively.

3. State estimation method

Assume the state-space form of the discrete-time system is written as follows:

$$\begin{cases} x_{k+1} = \mathbf{A}x_k + \mathbf{B}u_{1,k} + w_k \\ y_{k+1} = \mathbf{C}x_{k+1} + \mathbf{D}u_{2,k} + v_k \end{cases} \tag{8}$$

where x_k represents the state variable, $u_{1,k}$ and $u_{2,k}$ represents the system input, y_k represents the system output, w_k and v_k are the

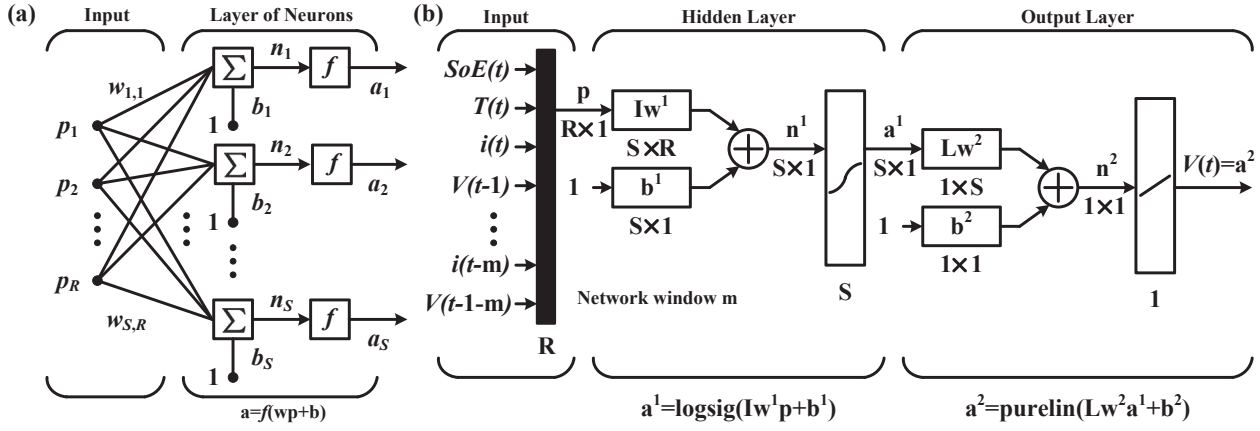

Fig. 3. (a) A single-layer network of $\boldsymbol{S}$ neurons having $\boldsymbol{R}$ inputs. (b) A network layer diagram which can be used as a general function approximator of cell voltage for SOE estimation.

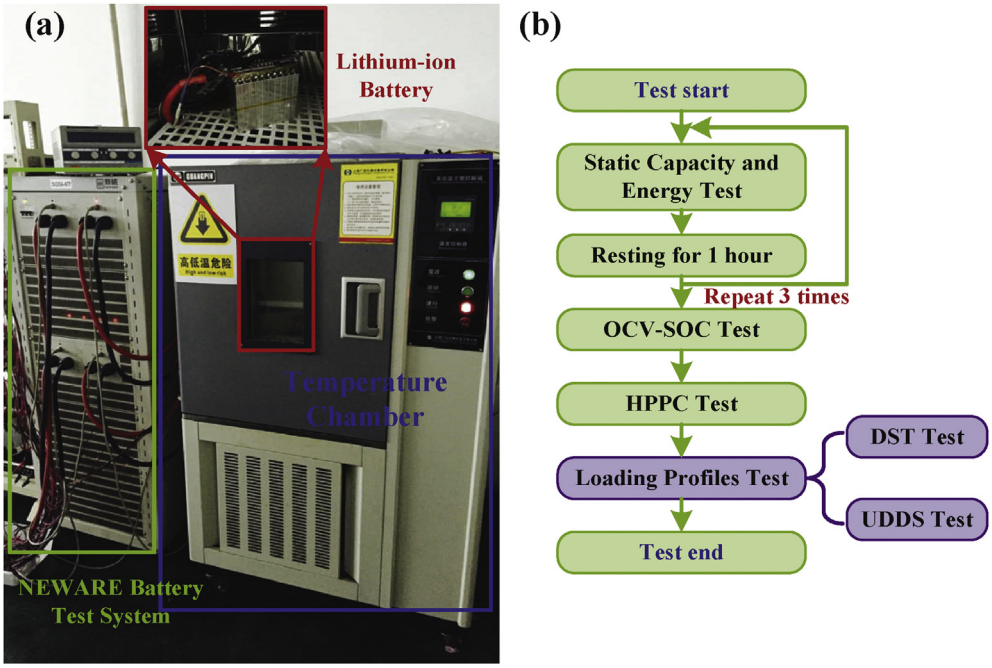

Fig. 4. (a) Configuration of battery test bench. (b) Battery test schedule.

Table 1
Test results of the static capacity and energy test.

	Cycle 1	Cycle 2	Cycle 3	Rated
Capacity(Ah)	99.025	98.886	98.829	100
Energy(Wh)	314.617	314.729	313.628	320

process noise and measurement noise, respectively.

The Bayesian learning technique using Monte Carlo simulation is considered in this work. Based on the probability approach, the system state is described as a probability density function $p(x_k|y_k)$ which can be approximated by particles that are generated from a priori distribution and updated from observations through a measurement model. The model parameters such as $U_{1,k}$, $U_{2,k}$, …, $U_{n,k}$ are included as a part of the state vector to be tracked. The detailed implementation of the probability based approach is summarized as follows:

Step 1 Randomly generate N initial particles on the basis of the probability density function $p(x_k|y_k)$. The particles approximate the distribution by:

$$p(x_k|y_{k-1}) = \sum_{i=1}^{N} \omega_{k-1}^{i} \left(\mathbf{A}x_{k-1}^{i} + \mathbf{B}u_{k-1} + w_{k-1} \right) \tag{9}$$

$$\omega_k^i = \omega_{k-1}^i p\left(y_k \middle| x_k^i\right) \tag{10}$$

where $p(y_k|x_k^i)$ is the likelihood of x_k^i. The likelihood is calculated as:

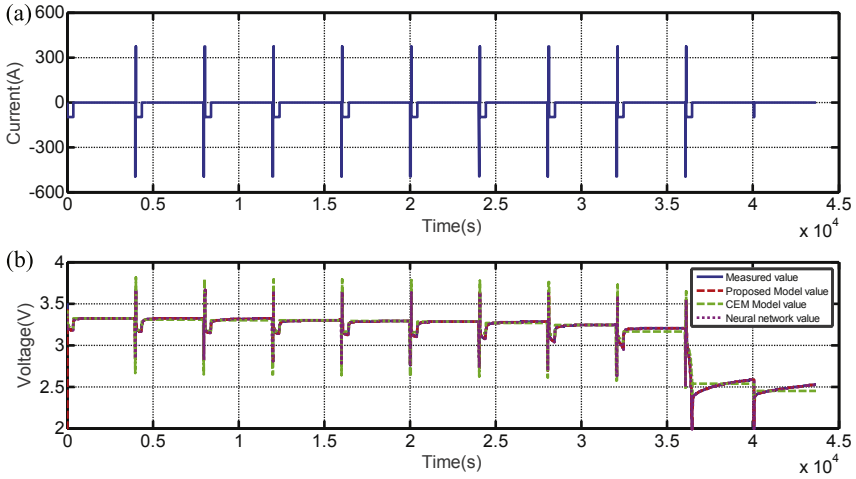

Fig. 5. The HPPC test: (a) Current profiles of the HPPC. (b) Voltage prediction based on different models.

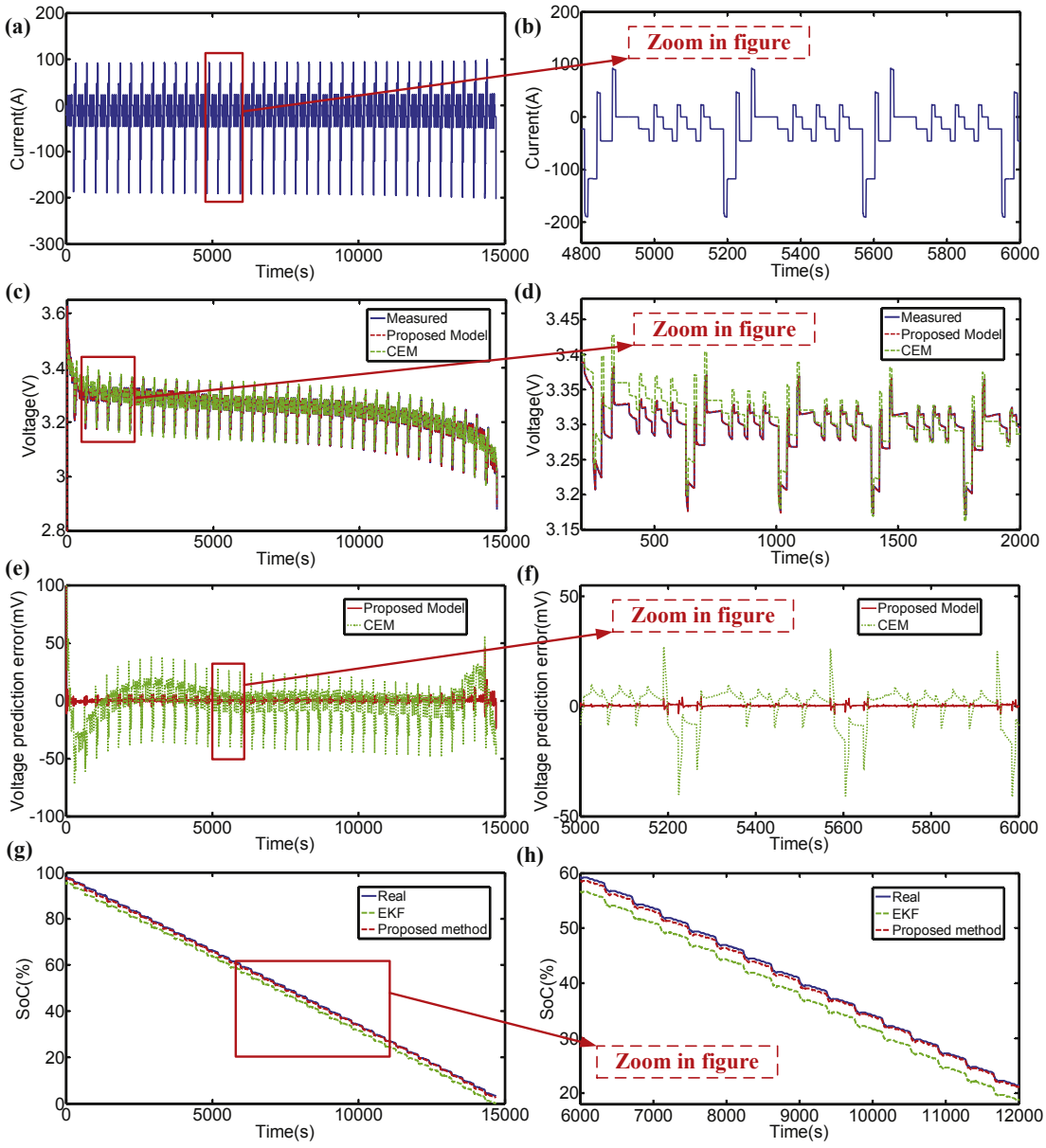

Fig. 6. The DST test for SOC estimation: (a) Current profiles of DST. (b) Zoom in figure of current profiles. (c) Comparison of the ECM and the proposed data-driven model. (d) Zoom in figure of the battery terminal voltage. (e) Comparison of the voltage prediction error. (f) Zoom in figure of the voltage prediction error. (g) Data-driven model based SOC estimation results using different estimation algorithms. (h) Zoom in figure of EKF and proposed method based SOC estimation results.

Table 2
Test results of the DST.

Method	MAEE(%)	RMSE(%)
Data-driven model based SOC estimation		
EKF	3.19	2.68
Proposed Method	0.97	0.53
Neural network model based SOE estimation		
EKF	3.96	2.75
Proposed Method	1.94	0.76

$$p\left(y_k\middle|x_k^i\right)=\frac{1}{\sqrt{2\pi\sigma^2}}\exp\left(-\frac{1}{2}\frac{(\hat{y}_k-y_k)^2}{\sigma^2}\right) \tag{11}$$

where σ is the standard deviation of the measurement noise v_k.

Then the overall weight of all samples can be normalized as:

$$\overline{\omega}_k^i=\omega_k^i\Big/\sum_{j=1}^{N}\omega_k^j \tag{12}$$

Step 2 Resampling: each particle is reserved or abandoned selectively according to its weight. This step can solve the problem of particle degeneracy to obtain a new set of the particles.

Step 3 Normalization: Calculate the overall weight of all samples and the estimation result is:

$$\hat{x}_k=\sum_{i=1}^{N}x_k^i\overline{\omega}_k^i \tag{13}$$

In the proposed method, the state distribution is represented by

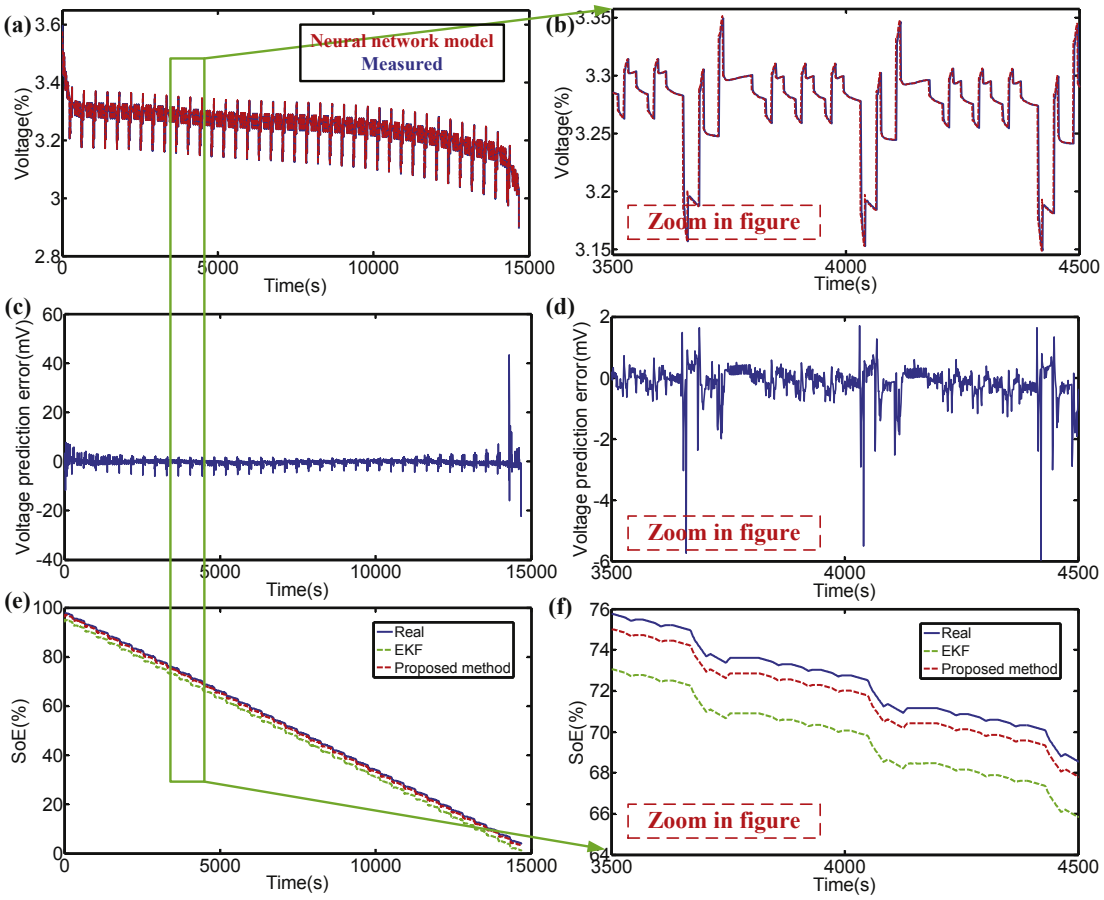

Fig. 7. The DST test for SOE estimation: (a) Voltage prediction result of the proposed neural network model. (b) Zoom in figure of the prediction result. (c) Voltage prediction error. (d) Zoom in figure of the voltage prediction error. (e) Neural network model based SOE estimation results using different estimation algorithms. (h) Zoom in figure of EKF and proposed method based SOE estimation results.

a set of samples. High probabilities are represented by a huge number of particles in a certain area, low probabilities by a low number or no particles in an area. Unlike the EKF based method, this approach uses a statistical approach which can yield better performance and works particularly well for nonlinear and robust problems. In addition, the system noise and observation noise are not limited to satisfy the Gaussian distribution by the proposed method.

4. Experiments and results analysis

4.1. Battery test bench and test schedule

In order to acquire experimental data such as current, voltage, temperature, accumulative Ah and Wh, etc., the battery test bench is established for the validation experiments. The configuration of the battery test bench is shown in Fig. 4 (a). The battery test bench includes a host computer, a NEWARE battery test system and a temperature chamber. The host computer is used for on-line experiment control and data recording. The battery test system is used to load the battery with programmable current profiles. The temperature chamber is used to provide manageable temperature.

Fig. 4 (b) shows the battery test schedule. All the training data sets and testing data sets are collected from the commercially available 1665130-type lithium-ion cells provided by Fujian Brother Electric CO., LTD of China. The static capacity and energy test is repeated three time for obtaining the average maximum available capacity and energy. The OCV-SOC test and the HPPC test are used for model parameter identification and model accuracy verification. Finally, the loading profiles tests are performed to verify the accuracy and robustness of the proposed method.

4.2. Static capacity and energy test

The maximum available capacity and energy test is performed to measure the maximum available capacity and energy of the battery. The maximum available capacity and energy of the battery are the number of ampere-hours and watt-hours that can be drawn from the battery at the nominal current, starting with the battery fully charged, which is maybe different with its nominal value due to the operation environment and aging levels. The available capacity and energy test is repeated three times and the average value is taken as the actual maximum available value. The test results are shown in Table 1. The rated capacity/energy of the tested battery is 100 Ah/320 Wh. The coulombic efficiencies of the three cycles are 99.259%, 99.216%, 99.373%, respectively. The energy efficiencies of the three cycles are 92.563%, 93.460%, 92.537%, respectively. The maximum available capacity/energy of the battery is 98.913 Ah/314.325 Wh.

4.3. Model prediction verification (HPPC test)

The HPPC test is used to verify the proposed model precision. The profiles of the HPPC are plotted in Fig. 5 (a). The data-driven

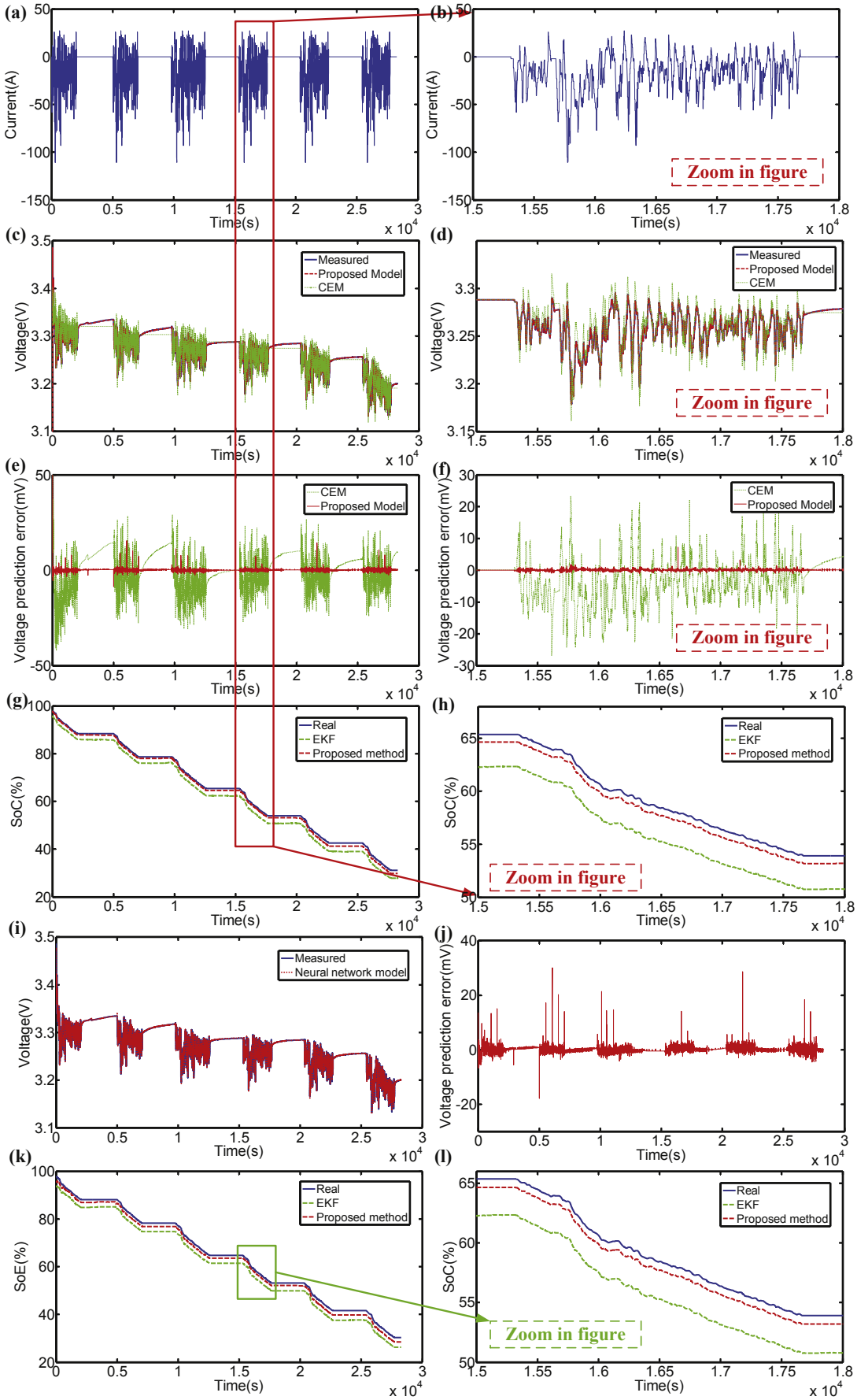

Fig. 8. The UDDS test results: (a) Current profiles of UDDS. (b) Zoom in figure of UDDS current profiles. (c) Comparison of the ECM and the proposed data-driven model. (d) Zoom in figure of the battery terminal voltage. (e) Comparison of the voltage prediction error. (f) Zoom in figure of the voltage prediction error. (g) Data-driven model based SOC estimation results using different estimation algorithms. (h) Zoom in figure of EKF and proposed method based SOC estimation results. (i) Voltage prediction result of the proposed neural network model. (j) Voltage prediction error of the neural network model. (k) Neural network model based SOE estimation results using different estimation algorithms. (l) Zoom in figure of EKF and proposed method based SOE estimation results.

Table 3
Test results of the UDDS.

Method	MAEE(%)	RMSE(%)
Data-driven model based SOC estimation		
EKF	3.62	3.05
Proposed Method	1.31	0.88
Neural network model based SOE estimation		
EKF	4.11	3.38
Proposed Method	2.12	1.54

model, neural network model and combined electrochemical model (CEM) are compared with the measured value as shown in Fig. 5 (b). As can be seen from the figure the data-driven model and the neural network model have higher prediction precision than the CEM with voltage error band of ± 10 mV and ± 20 mV under the HPPC profiles. The model precision is acceptable for SOC and SOE estimation.

4.4. Loading profiles test

In this work, the loading profiles tests include the DST and UDDS test are performed at 25 °C.

4.4.1. Dynamic Stress Test (DST)

In order to verify the accuracy and robustness of the proposed model and state estimation algorithm, the DST is performed on the selected battery. The dynamic current profiles are plotted in Fig. 6 (a) and (b) shows the zoom in figure. The model prediction precision of the proposed data-driven model is compared with the real measured value and the CEM in Fig. 6 (c) to (f). As can be seen from the figure, the voltage prediction error of the proposed model (± 8 mV error band) is much lower than that of the CEM (± 50 mV error band). The SOC estimation results and the zoom in figure are shown in Fig. 6 (g) and (h). The maximum absolute estimated error (MAEE) and the root mean square error (RMSE) are calculated to evaluate the estimation performance and the numerical results are shown in Table 2. As can be seen from the figure, the MAEE and RMSE for SOC estimation based on the proposed model and estimation algorithm are 0.97% and 0.53%, respectively. In contrast, the results based on EKF are 3.19% and 2.68%, respectively. The results show that the proposed method has accurate and robust estimation results in SOC estimation compared with the EKF method. Fig. 7 gives the DST testing results for SOE estimation. The model prediction of the proposed neural network model is shown in Fig. 7 (a) to (d). The SOE estimation results based on different estimation algorithms are shown in Fig. 7 (e) and (f). The MAEE and RMSE results of the EKF method for SOE estimation are 3.96% and 2.75%, respectively. Compared with the EKF method, the accuracy and robustness of the proposed method are much better with both the MAEE and RMSE under 2%.

4.4.2. Urban Dynamometer Driving Schedule (UDDS)

To further verify the accuracy and robustness of the proposed model and state estimation algorithm, the UDDS test is performed. The current profiles of the UDDS are shown in Fig. 8 (a) and (b) is the zoom in figure of one schedule. The model prediction precision of the proposed data-driven model is compared with the real measured value as shown in Fig. 8 (c) to (f). The voltage prediction error band of the neural network model is nearly ± 3 mV which is much lower than the ECM. The proposed model has shown excellent characteristic to approximate the real value. The SOC estimation results and the zoom in figure are shown in Fig. 8 (g) and (h). The MAEE and RMSE are shown in Table 3. As can be seen from the figure, the MAEE and RMSE for SOC estimation based on the data-driven model and estimation algorithm are 1.31% and 0.88%, respectively. And the results based on EKF are 3.62% and 3.05%, respectively. As a result, the performance of the proposed method is much better than the EKF under the UDDS profiles.

The model prediction results based on the proposed neural network under UDDS profiles is shown in Fig. 8 (i) and the prediction error is plotted in Fig. 8 (j). Finally, the SOE estimation results are compared in Fig. 8 (k) and (l) is the zoom in figure. The MAEE and RMSE results for SOE estimation based on the neural network model and the EKF are 4.11% and 3.38%, respectively. However, the probability based estimation algorithm shows better performance with MAEE and RMSE lower than 2.5% and 2%. As a result, accurate model prediction and robust estimation can be obtained by the proposed models and state estimation algorithm.

5. Conclusions

In this paper, we presented a probability based adaptive estimator for both SOC and SOE estimation. Accurate battery models are investigated based on data driven method and neural network. For the SOC estimation, an *n* ordered RC equivalent circuit model is employed by combining an electrochemical model to obtain more accurate voltage prediction results. For the SOE estimation, a sliding window neural network model is proposed to investigate the relationship between the terminal voltage and the model inputs. The HPPC test is performed to evaluate the model precision. The result indicates that accurate model prediction can be obtained by the proposed data-driven and neural network models with voltage error band of ± 10 mV and ± 20 mV, respectively. To verify the accuracy and robustness of the probability based state estimation algorithm, the DST and UDDS current profiles are performed on the commercial 1665130-type lithium-ion battery. The result shows that accurate and robust estimation of SOC and SOE can be obtained by the proposed algorithm with estimation error under 2.5%.

Acknowledgement

This work is supported by the National Natural Science Fund of China (Grant No. 61375079). We also appreciate the significant help of Fujian Brother Electric CO., LTD of China for supplying the test equipment and the lithium-ion batteries.

References

[1] J. Jiang, C. Zhang, Fundamentals and Application of Lithium-ion Batteries in Electric Drive Vehicles, John Wiley & Sons, 2015.
[2] L. Lu, X. Han, J. Li, et al., A review on the key issues for lithium-ion battery management in electric vehicles, J. Power Sources 226 (2013) 272–288.
[3] K.S. Ng, C.S. Moo, Y.P. Chen, et al., Enhanced coulomb counting method for estimating state-of-charge and state-of-health of lithium-ion batteries, Appl. Energy 86 (9) (2009) 1506–1511.
[4] Y. Xing, W. He, M. Pecht, et al., State of charge estimation of lithium-ion batteries using the open-circuit voltage at various ambient temperatures, Appl. Energy 113 (2014) 106–115.
[5] Y. Zheng, M. Ouyang, L. Lu, et al., Cell state-of-charge inconsistency estimation for $LiFePO_4$ battery pack in hybrid electric vehicles using mean-difference model, Appl. Energy 111 (2013) 571–580.
[6] I. Li, W. Wang, S. Su, et al., A merged fuzzy neural network and its applications in battery state-of-charge estimation, Energy Convers. IEEE Trans. 22 (3) (2007) 697–708.
[7] L. Xu, J. Wang, Q. Chen, Kalman filtering state of charge estimation for battery management system based on a stochastic fuzzy neural network battery model, Energy Convers. Manag. 53 (1) (2012) 33–39.
[8] M. Charkhgard, M. Farrokhi, State-of-charge estimation for lithium-ion batteries using neural networks and EKF, Ind. Electron. IEEE Trans. 57 (12) (2010) 4178–4187.
[9] W.X. Shen, C.C. Chan, E.W.C. Lo, et al., Adaptive neuro-fuzzy modeling of battery residual capacity for electric vehicles, Ind. Electron. IEEE Trans. 49 (3) (2002) 677–684.
[10] K.T. Chau, K.C. Wu, C.C. Chan, A new battery capacity indicator for lithium-ion battery powered electric vehicles using adaptive neuro-fuzzy inference

system, Energy Convers. Manag. 45 (11) (2004) 1681–1692.
[11] D.T. Lee, S.J. Shiah, C.M. Lee, et al., State-of-charge estimation for electric scooters by using learning mechanisms, Veh. Technol. IEEE Trans. 56 (2) (2007) 544–556.
[12] X. Tang, Y. Wang, Z. Chen, A method for state-of-charge estimation of $LiFePO_4$ batteries based on a dual-circuit state observer, J. Power Sources 296 (2015) 23–29.
[13] X. Hu, F. Sun, Y. Zou, Estimation of state of charge of a lithium-ion battery pack for electric vehicles using an adaptive Luenberger observer, Energies 3 (9) (2010) 1586–1603.
[14] B.S. Bhangu, P. Bentley, D.A. Stone, et al., Nonlinear observers for predicting state-of-charge and state-of-health of lead-acid batteries for hybrid-electric vehicles, Veh. Technol. IEEE Trans. 54 (3) (2005) 783–794.
[15] I.S. Kim, Nonlinear state of charge estimator for hybrid electric vehicle battery, Power Electron. IEEE Trans. 23 (4) (2008) 2027–2034.
[16] G.L. Plett, Extended Kalman filtering for battery management systems of LiPB-based HEV battery packs: part 1. background, J. Power Sources 134 (2) (2004) 252–261.
[17] G.L. Plett, Extended Kalman filtering for battery management systems of LiPB-based HEV battery packs. Part 2. Modeling and identification, J. Power Sources 134 (2) (2004) 262–276.
[18] G.L. Plett, Extended Kalman filtering for battery management systems of LiPB-based HEV battery packs: part 3. State and parameter estimation, J. Power Sources 134 (2) (2004) 277–292.
[19] R. Xiong, F. Sun, Z. Chen, et al., A data-driven multi-scale extended Kalman filtering based parameter and state estimation approach of lithium-ion polymer battery in electric vehicles, Appl. Energy 113 (2014) 463–476.
[20] Y. Wang, C. Zhang, Z. Chen, A method for state-of-charge estimation of Li-ion batteries based on multi-model switching strategy, Appl. Energy 137 (2015) 427–434.
[21] C. Hu, B.D. Youn, J. Chung, A multiscale framework with extended Kalman filter for lithium-ion battery SOC and capacity estimation, Appl. Energy 92 (2012) 694–704.
[22] G.L. Plett, Sigma-point Kalman filtering for battery management systems of LiPB-based HEV battery packs: part 1: introduction and state estimation, J. Power Sources 161 (2) (2006) 1356–1368.
[23] G.L. Plett, Sigma-point Kalman filtering for battery management systems of LiPB-based HEV battery packs: part 2: simultaneous state and parameter estimation, J. Power Sources 161 (2) (2006) 1369–1384.
[24] R. Xiong, X. Gong, C.C. Mi, et al., A robust state-of-charge estimator for multiple types of lithium-ion batteries using adaptive extended Kalman filter, J. Power Sources 243 (2013) 805–816.
[25] R. Xiong, F. Sun, X. Gong, et al., Adaptive state of charge estimator for lithium-ion cells series battery pack in electric vehicles, J. Power Sources 242 (2013) 699–713.
[26] H. He, R. Xiong, X. Zhang, et al., State-of-charge estimation of the lithium-ion battery using an adaptive extended Kalman filter based on an improved Thevenin model, Veh. Technol. IEEE Trans. 60 (4) (2011) 1461–1469.
[27] Y. Tian, B. Xia, W. Sun, et al., A modified model based state of charge estimation of power lithium-ion batteries using unscented Kalman filter, J. Power Sources 270 (2014) 619–626.
[28] W. He, N. Williard, C. Chen, et al., State of charge estimation for electric vehicle batteries using unscented Kalman filtering, Microelectron. Reliab. 53 (6) (2013) 840–847.
[29] Z. He, M. Gao, C. Wang, et al., Adaptive state of charge estimation for Li-ion batteries based on an unscented Kalman filter with an enhanced battery model, Energies 6 (8) (2013) 4134–4151.
[30] H. Gholizade-Narm, M. Charkhgard, Lithium-ion battery state of charge estimation based on square-root unscented Kalman filter, Power Electron. IET 6 (9) (2013) 1833–1841.
[31] Y. Wang, C. Zhang, Z. Chen, A method for joint estimation of state-of-charge and available energy of LiFePO4 batteries, Appl. Energy 135 (2014) 81–87.
[32] Y. Wang, C. Zhang, Z. Chen, A method for state-of-charge estimation of $LiFePO_4$ batteries at dynamic currents and temperatures using particle filter, J. Power Sources 279 (2015) 306–311.
[33] Y. He, X. Liu, C. Zhang, et al., A new model for state-of-charge (SOC) estimation for high-power Li-ion batteries, Appl. Energy 101 (2013) 808–814.
[34] G. Dong, J. Wei, C. Zhang, et al., Online state of charge estimation and open circuit voltage hysteresis modeling of $LiFePO_4$ battery using invariant imbedding method, Appl. Energy 162 (2016) 163–171.
[35] I.S. Kim, The novel state of charge estimation method for lithium battery using sliding mode observer, J. Power Sources 163 (1) (2006) 584–590.
[36] I.S. Kim, A technique for estimating the state of health of lithium batteries through a dual-sliding-mode observer, Power Electron. IEEE Trans. 25 (4) (2010) 1013–1022.
[37] X. Chen, W. Shen, Z. Cao, et al., A novel approach for state of charge estimation based on adaptive switching gain sliding mode observer in electric vehicles, J. Power Sources 246 (2014) 667–678.
[38] K. Mamadou, E. Lemaire, A. Delaille, et al., Definition of a state-of-energy indicator (SOE) for electrochemical storage devices: application for energetic availability forecasting, J. Electrochem. Soc. 159 (8) (2012) A1298–A1307.
[39] X. Liu, J. Wu, C. Zhang, Z. Chen, A method for state of energy estimation of lithium-ion batteries at dynamic currents and temperatures, J. Power Sources 270 (2014) 151–157.
[40] H. He, Y. Zhang, R. Xiong, et al., A novel Gaussian model based battery state estimation approach: state-of-energy, Appl. Energy 151 (2015) 41–48.
[41] G. Dong, X. Zhang, C. Zhang, et al., A method for state of energy estimation of lithium-ion batteries based on neural network model, Energy 90 (2015) 879–888.
[42] S. Piller, M. Perrin, A. Jossen, Methods for state-of-charge determination and their applications, J. power Sources 96 (1) (2001) 113–120.
[43] H. He, R. Xiong, H. Guo, et al., Comparison study on the battery models used for the energy management of batteries in electric vehicles, Energy Convers. Manag. 64 (2012) 113–121.